doi: **10.12029/gc20160419**

郑震, 陈衍景, 邓小华, 等. 东昆仑祁漫塔格地区白干湖钨锡矿田白云母$^{40}Ar/^{39}Ar$定年及地质意义[J]. 中国地质, 2016, 43(4): 1341−1352.

Zheng Zhen, Chen Yanjing, Deng Xiaohua, et al. Muscovite $^{40}Ar/^{39}Ar$ dating of the Baiganhu W-Sn orefield, Qimantag, East Kunlun Mountains, and its geological implications[J]. Geology in China, 2016, 43(4): 1341−1352(in Chinese with English abstract).

东昆仑祁漫塔格地区白干湖钨锡矿田白云母$^{40}Ar/^{39}Ar$定年及地质意义

郑 震[1] 陈衍景[1] 邓小华[2] 岳素伟[3] 陈红瑾[1]

(1.北京大学造山带与地壳演化重点实验室, 北京 100861; 2.北京矿产地质研究所, 北京 100012;
3.华南理工大学广州学院, 广东 广州 510802)

提要: 东昆仑祁漫塔格地区白干湖钨锡矿田是认识中国西北地区钨锡矿床成矿规律的重要窗口。作者对采自含矿石英脉的2个白云母样品进行$^{40}Ar/^{39}Ar$定年, 获得其坪年龄分别为(422.7±4.5) Ma和(421.8±2.7) Ma。2个样品的等时线年龄与反等时线年龄也在误差范围内一致, 分别为(424±15) Ma和(418±24) Ma, 表明分析数据可信。获得的白云母$^{40}Ar/^{39}Ar$坪年龄指示成矿作用发生在晚志留世, 与原特提斯洋闭合事件密切相关, 闭合后的陆陆碰撞使富含成矿物质的变质沉积物重熔而形成花岗岩浆; 花岗岩浆侵入并析出含矿热液, 导致钨锡成矿。

关 键 词: $^{40}Ar/^{39}Ar$定年; 白云母; 白干湖钨锡矿田; 祁漫塔格; 东昆仑造山带

中图分类号: P618.67;P618.44;P597 **文献标志码**: A **文章编号**: 1000−3657(2016)04−1341−12

Muscovite $^{40}Ar/^{39}Ar$ dating of the Baiganhu W−Sn orefield, Qimantag, East Kunlun Mountains, and its geological implications

ZHENG Zhen[1], CHEN Yan−jing[1], DENG Xiao−hua[2], YUE Su−wei[3], CHEN Hong−jin[1]

(1.*Key Laboratory of Orogen and Crust Evolution, Peking University, Beijing* 100871*, China;* 2.*Beijing Institute of Geology for Mineral Resources, Beijing* 100012*, China;* 3.*Guangzhou College, South China University of Technology, Guangzhou* 510802*, Guangdong China*)

Abstract: The newly discovered Baiganhu W−Sn ore district in Qimantag of East Kunlun orogenic belt provides a key window to insight into the W−Sn mineralization in Northwest China. In this paper, the authors present results from the $^{40}Ar/^{39}Ar$ dating of two muscovite samples collected from the ore−bearing quartz veins in the Baiganhu W−Sn ore district, which yielded two $^{40}Ar/^{39}Ar$ plateau ages of 422.7 ± 4.5 Ma and 421.8 ± 2.7 Ma, respectively. These two samples also yielded consistent (within errors) isochronal and inverse isochronal ages of 424 ± 15 Ma and 418 ± 24 Ma, respectively, suggesting that the analytical results are reliable. The new plateau ages show that the mineralization occurred in the Late Silurian, associated with the tectonic−thermal

收稿日期:2016−03−14;**改回日期**:2016−06−20

基金项目:中国地质调查局项目"环塔里木前寒武纪铜镍−钨锡矿成矿规律及找矿方向"(1212011140056)资助。

作者简介:郑震,女,1987年生,博士生,研究方向为矿床学、岩石学、矿物学;E−mail:tianchilian@163.com。

通讯作者:陈衍景,男,1962年生,教授,研究方向为矿床学、造山带成矿规律;E−mail:yjchen@pku.edu.cn。

events induced by the closure of Proto−Tethys. The post−subduction continental collision caused the formation of granitic magmas sourced from re− melting of the metalliferous metamorphosed Proterozoic sediments. The W− Sn mineralization resulted by the hydrothermal fluids exsolved from the granitic magmas during their upward emplacement.

Key words: $^{40}Ar/^{39}Ar$ dating; muscovite; Baiganhu W−Sn ore district; Qimantag; East Kunlun orogenic belt

About the first author: ZHENG Zhen, female, born in 1987, doctor, mainly engages in the study of mineral deposits, petrology and mineralogy; E−mail: tianchilian@163.com.

About the corresponding author: CHEN Yan−jing, male, born in 1962, professor, engages in the study of mineral deposits, ore−forming regularity of orogenic belt; E−mail: yjchen@pku.edu.cn.

Fund support: Supported by China Geological Survey Project (No. 1212011140056).

昆仑山脉是中国中央造山带的重要组成, 被阿尔金断裂分割为东昆仑造山带与西昆仑造山带两部分。东昆仑造山带北邻塔里木地块和柴达木地块, 南邻巴颜喀拉地体, 东与秦岭造山带相接, 延绵大于1000 km。以其曼于特断裂和昆中断裂为界, 东昆仑造山带可进一步划分为祁漫塔格(昆北地体), 昆中地体与昆南地体。其中, 祁漫塔格主体形成于原特提斯洋的闭合过程[1−11](图1−a, b)。

祁漫塔格地区的白干湖钨锡矿田发现于2002年, 它是国内少有的加里东造山期形成的大型钨锡矿田, 不同于华南燕山期钨锡矿集区[12]。白干湖钨锡矿田为研究中国西北地区钨锡矿床成矿规律, 高效实施成矿预测和找矿勘查, 提供了一个重要窗口, 因此, 其研究备受学者重视。前人研究已经获得了白干湖矿田成矿岩体的锆石U−Pb年龄[13−14], 确定了流体包裹体温度及成矿流体的性质[15−16], 但成矿年龄尚未得到精确厘定。

云母类矿物的$^{40}Ar/^{39}Ar$定年是确定热液矿床成矿年龄的最有效手段之一, 被广泛应用于确定多类矿床的成矿时代, 如金矿床[17−18]、铀矿床[19−20]、钨锡矿床[21−26]。白干湖钨锡矿田含矿石英脉两侧脉壁较好发育了热液白云母线, 笔者挑选了与矿石密切共生的白云母进行$^{40}Ar/^{39}Ar$定年, 获得了精确的年龄, 较好厘定了成矿时代, 据此探讨了白干湖钨锡矿田的成因, 特此报道。

1 区域地质

祁漫塔格地区位于东昆仑造山带北部, 北邻柴达木地块, 南以其曼于特断裂为界, 西以阿尔金断裂为界(图1−b)。区内地层以元古宇金水口群为基

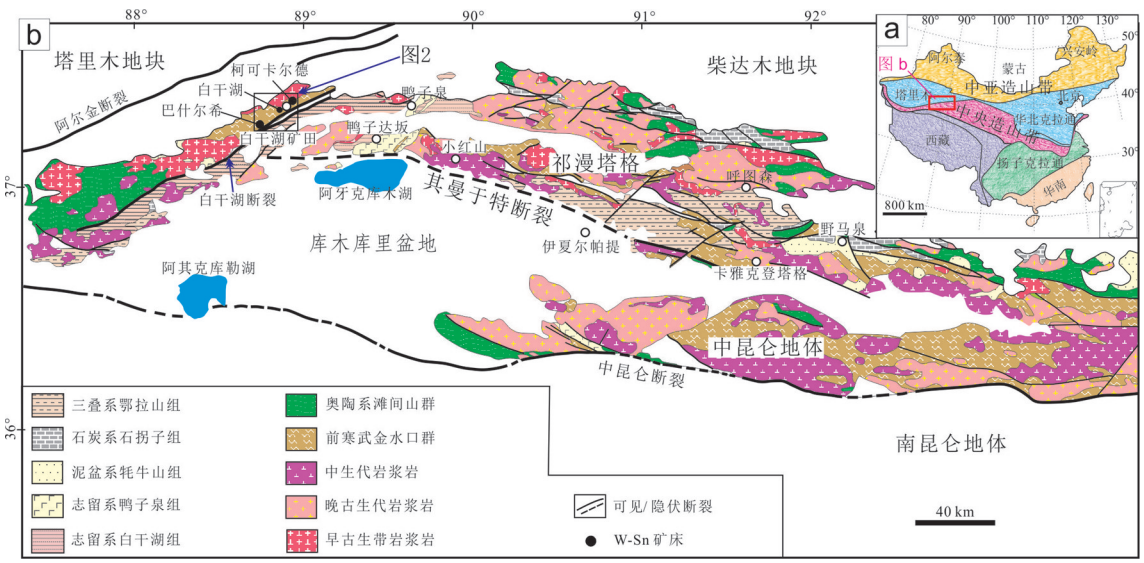

图1 祁漫塔格区域地质图[28]

Fig. 1 Location and regional geology of the Qimantag area[28]

底, 其上不整合覆盖下古生界滩间山群及泥盆系牦牛山组, 石炭系石拐子组和三叠系鄂拉山组[27−30]。

金水口群自下而上依次为古元古界白沙河组, 中元古界小庙组和狼牙山组, 新元古界丘吉东沟组。白沙河组是一套片岩、大理岩、混合岩、角闪岩组合; 小庙组主要含石英岩、大理岩、片麻岩、白云母石英片岩[31]; 狼牙山组主要由一套白云岩、灰岩、砂岩、页岩组成, 含叠层石化石*Jacutophyton sp*., 是确定地层时代的依据之一; 丘吉东沟组含碎屑岩、硅质岩、镁质碳酸盐, 含叠层石化石*Spicaphytonqiujidonggouense* [32]。滩间山群是一套碎屑岩、火山岩夹碳酸盐序列, 岩性主要为千枚岩、变质砂岩、片岩、粉砂岩、安山岩、凝灰岩、大理岩、白云岩, 含植物化石*Leiospaeridie sp*., *Micrhystridium sp*., 珊瑚化石*Heliolites sp*., *Rhabdotetvadiumqinghaiense*, 以及笔石化石*Monograptuspriodon* (*Bronn*), *Monograptus sp*., *Streptograptus cf. becki* (*Barrande*), 形成年代为中奥陶世至志留纪。最近, 李荣社等[28]从滩间山群中解体出志留系白干湖组和鸭子泉组。白干湖组是一套复理石建造, 前者仅沿白干湖断裂东侧分布; 鸭子泉组是一套中基性岛弧火山岩建造, 以构造块体形式出露于鸭子泉—鸭子达坂一带[29, 33−35]。晚泥盆世牦牛山组是一套磨拉石建造, 含腕足类化石[36]。早石炭世石拐子组主要含碎屑岩和碳酸盐岩, 产珊瑚化石和腕足类化石。鄂拉山组则主要为一套火山碎屑岩[29, 37−38]。

祁漫塔格地区经历了多期构造事件, 主要为晋宁期和加里东期。区内发育NW、NNW走向的断裂、褶皱及剪切带, 而NE走向的韧性剪切带则主要在鸭子泉一带[39−40]。其曼于特逆断裂是祁漫塔格地区的主断裂, 控制了区内地层及侵入岩的分布, 形成于早古生代。主断裂面南倾, 倾角为50°~70°, 沿断裂带发育挤压破碎带[41−42]。祁漫塔格地区广泛出露古生代至中生代侵入体, 元古宙侵入体较少。侵入体以花岗岩类为主, 呈岩基或岩株沿其曼于特断裂分布, 岩性主要为黑云母花岗岩、二长花岗岩、钾长花岗岩[43−45]。

2　矿田地质

白干湖钨锡矿田是秦祁昆成矿带的西延(图2), 位于祁漫塔格最西部, 包含巴什尔希, 白干湖, 柯可卡尔德3个矿床, 钨锡储量分别为174913 t和79091 t[14, 46−48](图2)。矿区出露地层主要是中元古界小庙组和志留系白干湖组。白干湖断裂是矿区主要断裂, 全长230 km, 表现为宽2.5~5 km的舒缓波状挤压片理化带, 呈NE−SW走向, 倾向SE, 倾角70°~80°。断裂带中分布的新元古界丘吉东沟组强烈糜棱岩化, 矿区内其他断裂和褶皱轴基本与白干湖断裂平行[46]。矿区内出露的岩浆岩为加里东期二长花岗岩和钾长花岗岩, 分布于矿田北侧及西侧。钨锡矿化类型分3种: 矽卡岩型, 云英岩化花岗岩细网脉浸染型(云英岩型), 石英脉型(图3−a)。矽卡岩型及云英岩型矿体主要产于二长花岗岩体顶部接触带, 矿体呈层状, 透镜状产出, 并且云英岩型矿体部分叠加于矽卡岩型矿体。石英脉型矿体产于岩体顶部外接触带金水口群中, 部分矿脉产于矽卡岩及云英岩。围岩蚀变以矽卡岩化、云英岩化、硅化为主[49]。巴什尔希矿床以矽卡岩型和石英脉型为主, 矿体长800~3600 m, 厚度1.2~22.5 m, 走向60°~90°, 倾向SE, 倾角35°~85°。白干湖矿床以矽卡岩型和云英岩型为主, 矿体一般长180~800 m, 最长可达1300 m, 厚度5~60 m, 走向40°~87°, 倾向SE, 倾角70°~80°。柯可卡尔德矿床以石英脉型和云英岩型为主, 矿体长50~250 m, 厚度1.3~43 m, 走向50°~60°, 倾向SE, 倾角20°~60°[14, 46, 49]。

根据野外地质观察, 结合岩相学及矿脉矿物组合, 将白干湖矿田矿化期分为4阶段, 3种矿化类型的主成矿期均为第一阶段。在第一阶段, 矽卡岩型矿化主要形成半自形−他形粒状白钨矿, 少量锡石, 脉石矿物则以透辉石、黝帘石、透闪石、榍石、石英为主。云英岩型及石英脉型矿体的矿石矿物以黑钨矿和锡石为主, 黑钨矿呈自形板状或团块状, 锡石为常见双晶及环带的自形−半自形粒状, 可见少量白钨矿及金属硫化物细脉; 脉石矿物主要为石英、白云母、电气石, 石英脉两侧发育厚约1 cm的白云母线。第二阶段主要形成白钨矿, 呈他形粒状晶形, 或交代黑钨矿, 或呈细脉浸染状穿切黑钨矿及锡石; 脉石矿物主要含石英、电气石、磷灰石, 伴随少量金属硫化物细脉。第三阶段是金属硫化物阶段, 是黄铁矿、黄铜矿、磁黄铁矿、毒砂等金属硫化物大量沉淀的阶段, 含少量独居石。第四阶段是无

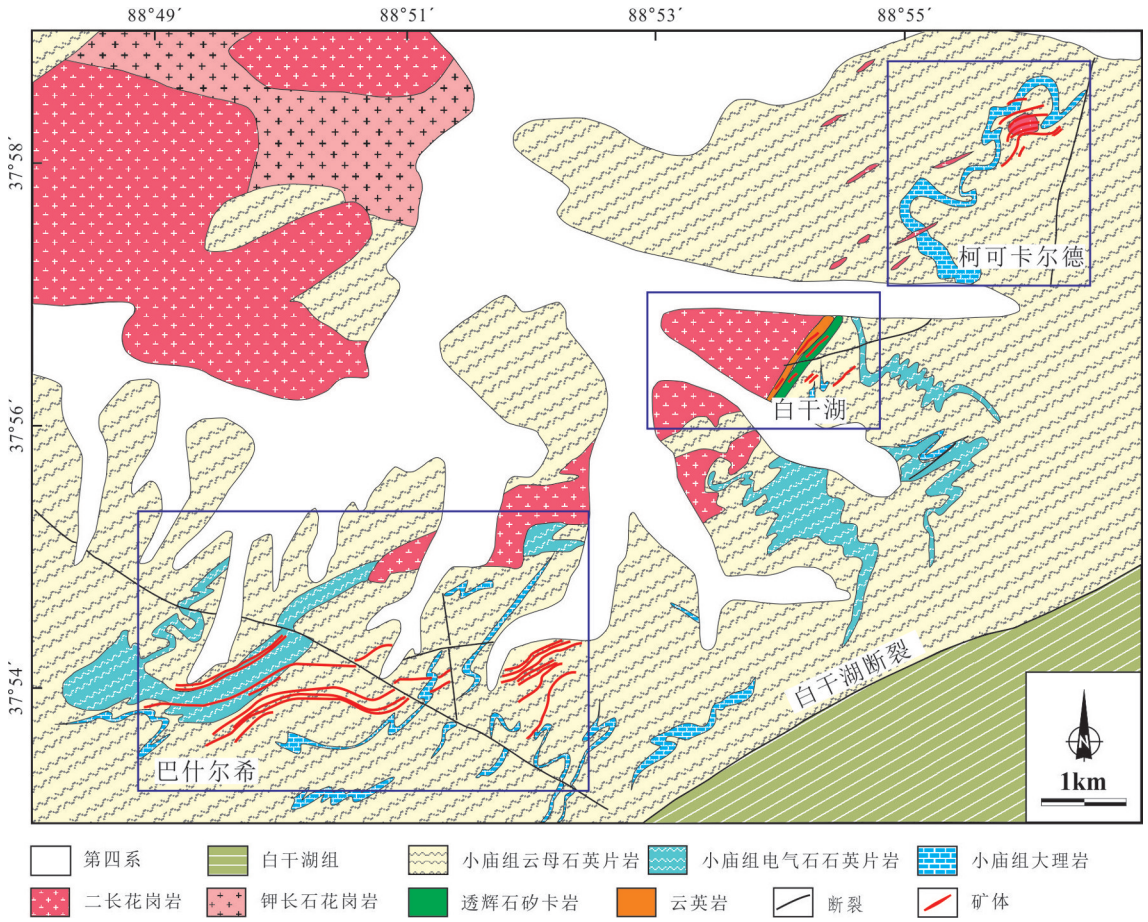

图2 白干湖钨锡矿田地质图[14]

Fig.2 Geological map of the Baiganhu W−Sn ore district[14]

矿阶段, 主要矿物为石英、方解石、萤石。

3 样品及分析方法

白云母在白干湖钨锡矿田内广泛发育。本次研究选取BW−13和KA−13两个样品, 其中BW−13取自巴什尔希钻孔ZK1202, 深度为236 m, KA−13采自地表, 均为含矿石英脉与围岩接触带的云母线。云母线可达1 cm, 白云母呈较自形板状产出, 与锡石、黑钨矿等矿石密切共生(图3−b, c, d)。单偏光下观察表面发育一组节理, 未见蚀变, 正交光下显示二级蓝绿干涉色(图3−e, f)。

将白云母样品粉碎筛选后, 经过水漂, 磁选, 重液分离等过程, 分选出80目的云母颗粒, 然后在双目镜下挑选出高纯度(大于99 %)白云母。将挑出的白云母先后用超声波, 蒸馏水及丙酮清洗, 清除白云母吸附的粉尘及有机杂质。

白云母中子照射在中国原子能科学研究院49−2反应堆B4孔道进行。用纯铝铂纸将0.18~0.28 mm粒径的白云母样品包成直径6 mm球形, 封闭于石英玻璃瓶中。照射时长为24 h 14 min, 快中子通量为2.2576×10^{18}。用于中子通量检测的样品为ZBH−25 (年龄为132.7 Ma)。同时对纯物质CaF_2和K_2SO_4进行同步照射, 得出校正因子为:$(^{36}Ar/^{37}Ar)_{Ca}$=0.000271, $(^{39}Ar/^{37}Ar)_{Ca}$ = 0.000652, $(^{40}Ar/^{39}Ar)_{k}$ = 0.00703。照射后的样品经冷却, 装入样品架中经密封去气后, 装入系统。

白云母Ar/Ar定年测试于北京大学造山带与地壳演化教育部重点实验室常规$^{40}Ar/^{39}Ar$定年系统进行。采用钽(Ta)熔样炉进行阶步升温熔样, 每个样品分为10~14步加热释气, 温阶范围为800~1500 ℃, 每个加热点在恒温状态下保持20 min。系统分别采用海绵钛炉(20 min)、活性炭冷井(10 min)

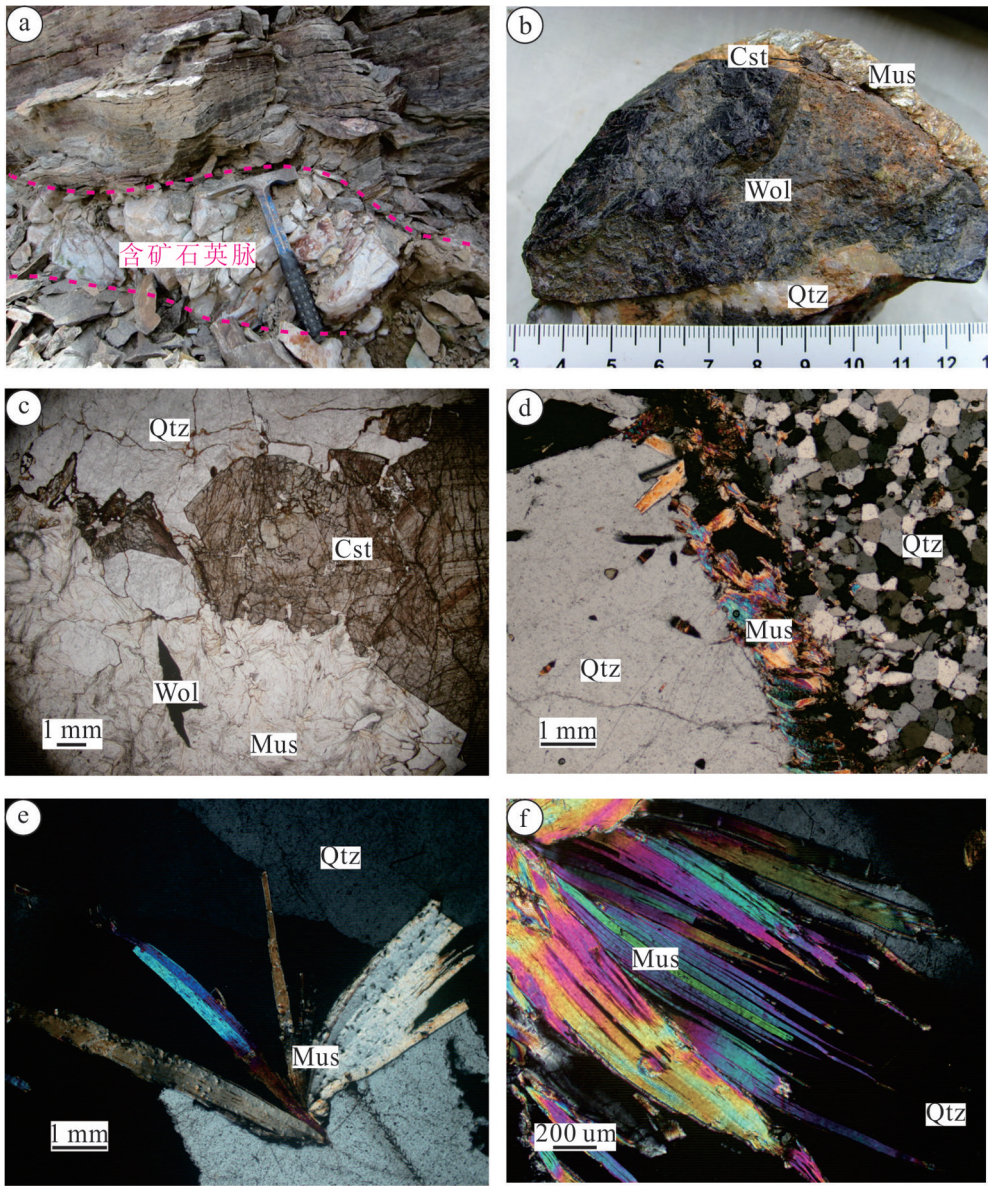

图3 白干湖钨锡矿田白云母产状及岩相图

a—含矿石英脉侵入云母石英片岩, 白云母十分发育; b—云母线在含矿石英脉壁上产出; c—单偏光下观察, 白云母在含矿石英脉一侧十分发育, 与锡石、黑钨矿密切共生; d—块状含矿石英脉侵入围岩后, 使围岩发生硅化, 生成细粒石英, 并且在接触带发育云母线; e, f—白云母集合体, 正交偏光下具有二级蓝绿干涉色;

Cst—锡石; Mus—白云母; Qtz—石英; Wol—黑钨矿

Fig.3 Modes of occurrence and petrography of muscovite in the Baiganhu W−Sn ore district

a−Ore−bearing quartz veins intruding the mica−quartz schist, containing muscovite; b− Muscovite occurring along the ore−bearing quartz veins; c− Muscovite coexisting with cassiterite and wolframite (plainlight); d−Ore−bearing quartz vein intruding the wall rocks which were replaced by fine−grain quartz; e and f− Muscovite aggregates (crossed nicols).

Mineral abbreviations: Cst−Cassiterite; Mus−Muscovite; Qtz−Quartz; Wol−Wolframite

及锆钒铁吸气剂炉(15 min)对气体进行纯化。使用RGA10型质谱仪记录5组Ar同位素信号, 信号强度单位为Mv。质谱峰循环测定9次, 用峰顶值减去前后基线的平均值来获得Ar同位素数据。数据处理采用$^{40}Ar/^{39}Ar$ Dating 1.2对各组数据进行校正计算, 再采用Isotope 3.0计算坪年龄及等时线年龄[50]。测

试样品放射性成因^{40}Ar很高, 所以坪年龄可以参考。坪年龄计算据Dalrymple et al.提出的标准计算[51], 即存在不少于3个加热阶段且释放^{39}Ar大于50%。

4 定年结果

白云母的阶段加热^{40}Ar/^{39}Ar定年数据列于表1。其中, BW−13样品共11个加热阶段, 温度变化区间为900~1400 ℃; KA−13样品共10个加热阶段, 温度变化区间为900~1350 ℃。白云母阶段升温年龄图谱及坪年龄见图4−a, d, 所有构成坪年龄的数据点绘制对应等时线及反等时线图(图4−b, c; 4−e, f)。受核反冲和测量误差影响, 在BW−13年龄谱线左侧及右侧出现了6个不一致视年龄值, KA−13则出现了5个不一致视年龄值, 但其所占比例较少, 参与加权平均年龄计算的温阶累计^{39}Ar释放量达到68 %和60.8 %, 加权平均年龄分别为(422.7±4.5) Ma, (421.8±2.7) Ma。BW−13与KA−13样品中, 参与加权平均年龄的5个点构成一条十分吻合的等时线, 其等时线年龄分别为(424±15) Ma及(418±24) Ma, 与反等时线年龄一致。初始^{40}Ar/^{36}Ar比值则分别为231及580, 与尼尔值 (295.5±5) 有差距。白云母的Ar对后期地质作用很敏感, 即使少部分受到后期地质作用的叠加改造, 白云母也可以形成明显的扩散丢失图谱, 未受扰动的白云母则形成平坦的年龄谱[52−58] 。本次测试的BW−13及KA−13两个样品的年龄谱均平坦无异常, 且各数据点呈较好的线性关系, 说明白云母形成以后未受到后期热事件的扰

表1 白干湖钨锡矿田白云母^{40}Ar/^{39}Ar阶段升温定年结果

Table 1 ^{40}Ar/^{39}Ar stepwise heating dating of muscovite from the Baiganhu W−Sn orefield

温阶	T/℃	年龄/Ma	±2σ	^{40}Ar*/%	^{39}Ar/Mols	^{40}Ar/^{39}Ar	±2σ	^{38}Ar/^{39}Ar	±2σ	^{37}Ar/^{39}Ar	±2σ	^{36}Ar/^{39}Ar	±2σ	^{40}Ar*/^{39}Ar	±2σ
BW−13, *J*=0.004783															
01	900	186.71	11.58	67.34	3.01E-10	33.85	1.39	0.067	0.002	0.925	0.034	0.037	0.002	22.797	1.478
02	950	386.71	7.11	90.71	6.69E-10	55.09	0.70	0.017	0.007	0.052	0.020	0.017	0.002	49.981	0.948
03	1000	420.84	3.20	96.42	1.85E-09	56.96	0.21	0.023	0.003	0.177	0.000	0.007	0.000	54.928	0.213
04	1050	424.31	2.94	98.85	2.94E-09	56.07	0.03	0.015	0.000	0	0	0.002	0.000	55.438	0.099
05	1100	423.92	3.41	98.64	3.21E-09	56.14	0.22	-0.012	0.001	0.097	0.001	0.003	0.001	55.380	0.271
06	1150	422.83	2.93	98.98	2.64E-09	55.78	0.08	0.013	0.003	0.087	0.001	0.002	0.000	55.221	0.094
07	1200	421.54	3.39	98.96	2.14E-09	55.60	0.03	0.007	0.004	0	0	0.002	0.001	55.031	0.269
08	1250	403.63	3.41	95.8	1.47E-09	54.74	0.26	0.018	0.001	0.204	0.004	0.008	0.000	52.422	0.293
09	1300	403.25	2.74	97.80	1.29E-09	53.54	0.01	0.004	0.009	0.163	0.003	0.004	0.000	52.367	0.013
10	1350	396.18	2.86	99.70	1.19E-09	51.49	0.06	0.011	0.004	0.027	0.008	0.001	0.000	51.345	0.138
11	1400	349.07	2.97	93.40	1.09E-09	47.78	0.24	0.016	0.000	0.366	0.002	0.011	0.000	44.632	0.245
KA−13, *J*=0.004784															
01	900	360.84	32.07	77.19	1.17E-10	59.95	4.49	0.19	0.016	2.37	0.190	0.046	0.001	46.283	4.502
02	950	387.08	19.74	95.29	2.33E-10	52.49	2.33	0.03	0.002	0	0	0.008	0.005	50.023	2.766
03	1000	422.79	5.51	98.30	1.08E-09	56.15	0.30	0.01	0.008	0.10	0.004	0.003	0.001	55.202	0.424
04	1050	425.64	4.78	98.85	2.49E-09	56.26	0.09	0.02	0.003	0.06	0.003	0.002	0.000	55.620	0.112
05	1100	421.44	4.77	99.05	3.27E-09	55.52	0.12	0.01	0.003	0	0	0.002	0.000	55.005	0.135
06	1150	420.52	4.67	99.12	3.36E-09	55.35	0.01	0.01	0.001	0.08	0.000	0.002	0.000	54.870	0.024
07	1200	419.05	4.73	99.20	3.64E-09	55.09	0.09	0.01	0.003	0.06	0.002	0.001	0.000	54.656	0.124
08	1250	413.61	4.61	99.2	3.74E-09	54.28	0.04	0.02	0.002	0.05	0.000	0.001	0.000	53.862	0.045
09	1300	386.99	5.07	98.40	2.97E-09	50.82	0.01	0.01	0.004	0.06	0.002	0.003	0.001	50.012	0.379
10	1350	371.82	4.25	98.28	1.87E-09	48.67	0.05	0.01	0.000	0.161	0.002	0.003	0.000	47.842	0.110

注: *代表放射性成因^{40}Ar。

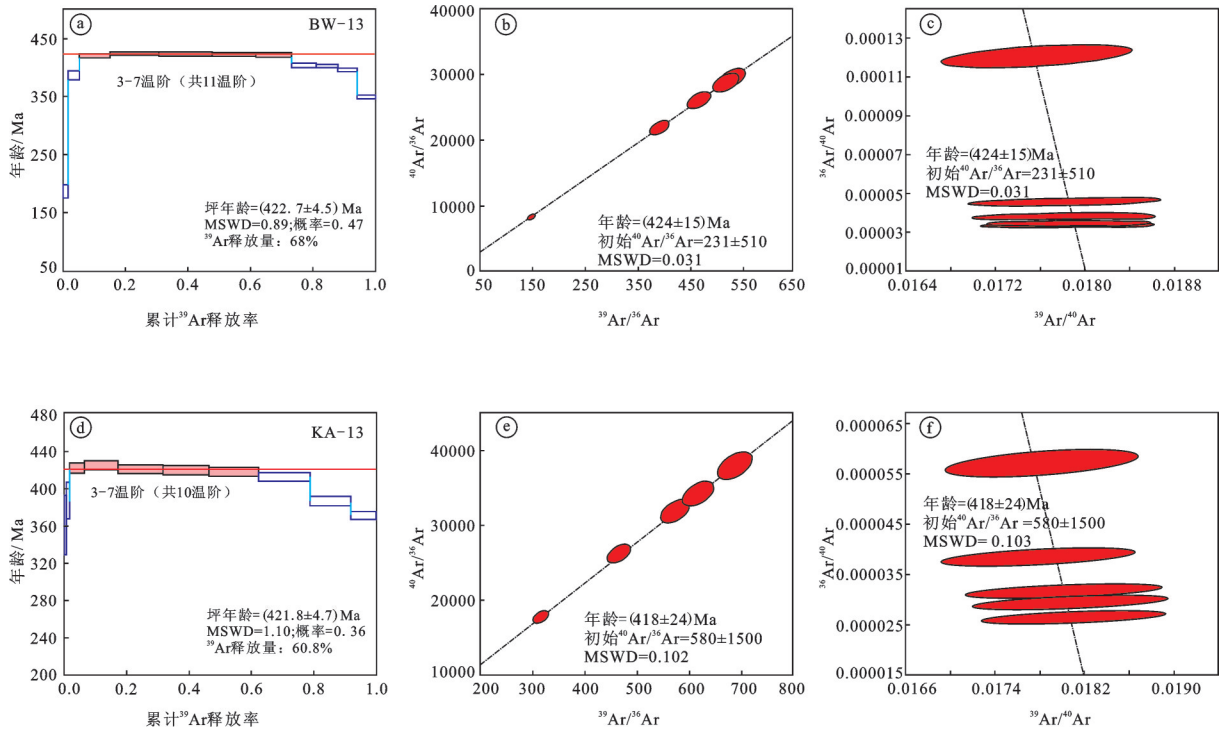

图4 白干湖矿田白云母$^{40}Ar/^{39}Ar$年龄谱, 等时线及反等时线年龄图

Fig.4 $^{40}Ar/^{39}Ar$ age spectra, isochronal and inverse isochronal age of muscovite from the sample of the Baiganhu W-Sn ore district

动。2个样品的坪年龄与等时线年龄、反等时线年龄在误差范围内一致, 说明白云母的$^{40}Ar/^{39}Ar$定年结果是可靠且具有地质意义。因此, 本次获得白云母421.8和422.7 Ma的$^{40}Ar/^{39}Ar$坪年龄可以代表其形成后冷却至其Ar同位素体系封闭温度时的年龄[53-59]。

5 讨　论

5.1 成矿时代

白云母相对黑云母及金云母较稳定, 其晶体结构有利于Ar的保存, 使Ar不易丢失, 其Ar-Ar定年结果可能代表矿物的结晶年龄, 也可能是矿物被后期地质事件改造的年龄[53-54, 58-64]。本文所测2个白云母样品在形成之后均未受到后期构造热事件的影响, 所获白云母冷却年龄可以代表其结晶年龄。

矿石中含钾蚀变矿物及成矿流体的Ar-Ar年龄是确定热液矿床成矿时期的重要方法[60-67]。本文中用于Ar-Ar测年的白云母样品与锡石及黑钨矿密切共生, 在矿脉与围岩交界处形成白云母线, 证明该白云母是主成矿期产物。白云母K-Ar同位素体系的封闭温度为(350±50) ℃[53, 59, 66], 这与前人所测含矿石英脉流体包裹体均一温度一致[15-16], 表明该矿床中白云母的$^{40}Ar/^{39}Ar$年龄可以代表成矿年龄。因此, 样品BW-13及KA-13的坪年龄(422.7±4.5) Ma和(421.8±2.7) Ma代表了白干湖钨锡矿田的成矿时间。该年龄值略晚于矿田内巴什尔希二长花岗岩体的侵入时代(431±1 Ma), 与锡石LA-ICP-MS方法获得U-Pb年龄(427±13 Ma)在误差范围内一致[13-14], 说明成矿发生在岩浆期后的热液作用过程中。

5.2 矿床成因

前人研究获得白干湖矿田含矿石英脉$\delta^{18}O_{H2O}$值为4.02‰~6.32‰, δD值为-75.5‰~ -42.8‰, 与原始岩浆水一致, 表明成矿流体来自于岩浆热液[16]。对白干湖矿床含矿石英脉中电气石B同位素及地球化学分析, 也表明成矿流体来源于变质沉积物重熔形成的花岗岩浆[68]。

巴什尔希花岗岩体呈岩基、岩株状或岩脉侵入金水口群小庙组, 主要出露于矿区北侧及西侧, 面积约200 km^2, 岩性主要为二长花岗岩及钾长花岗岩。野外地质观察发现, 白干湖钨锡矿田内矽卡岩

型及云英岩型矿体主要产于二长花岗岩与围岩接触带, 石英脉型矿体产于隐伏二长花岗岩顶部外接触带的小庙组中。其中, 柯可卡尔德矿床有大量矿体产于隐伏二长花岗岩顶部, 并且二长花岗岩W、Sn含量较高, 说明白干湖钨锡矿区内与成矿密切相关的岩体是二长花岗岩[49, 69]。通过岩相学观察, 二长花岗岩的主要组分为石英、斜长石、钾长石、白云母, 少量黑云母。副矿物含电气石、钛铁矿、榍石、石榴石、绿泥石、磷灰石、锆石。二长花岗岩的主量元素及微量元素特征表明其属于S型花岗岩[13, 70]。此外, 前人获得二长花岗岩锆石Hf同位素二阶段模式年龄(T_{DM2})为1061~1561 Ma, 认为其源区物质属中元古代[13], 与中元古界金水口群一致。金水口群地层W浓度克拉克值达15.8, 丰度平均值为20.5×10^{-6}, Sn浓度克拉克值为1.3, 丰度平均值为3.3×10^{-6}。因此, 中元古界金水口群可为白干湖钨锡矿田形成提供了成矿金属[46, 49, 70]。总之, 白干湖钨锡矿田含矿流体来自于中志留世的巴什尔希二长花岗岩体, 而该岩体由中元古代金水口群的变质沉积物重熔形成。

研究区在新元古代至早古生代位于原特提斯洋北缘, 并具有多岛洋盆的特点[71−76]。期间, 原特提斯洋向北俯冲形成昆中岛弧、祁漫塔格弧后盆地[28, 34−35, 77]。早古生代末期(中志留世)原特提斯洋闭合, 祁漫塔格(昆北地体)、昆中、昆南地体先后向北拼接于塔里木—柴达木地块[27, 35, 77−80]。碰撞引起祁漫塔格地区上地壳泥质沉积物(主体为金水口群)重熔, 形成富含钨锡的二长花岗岩侵入体, 在侵入体内外接触带形成矽卡岩型及云英岩型矿化类型, 在外接触带至围岩裂隙及层间断层构造发育石英脉型矿化, 且沿脉壁两侧发育白云母线。

6 结 论

(1)白干湖钨锡矿田与矿石密切共生的白云母$^{40}Ar/^{39}Ar$坪年龄为(421.8±2.7)~(422.7±4.5) Ma, 可以代表成矿年龄, 属晚志留世。

(2)志留纪时原特提斯洋的消亡导致昆北地体与塔里木—柴达木地块拼贴碰撞, 引起祁漫塔格地区中元古代富含钨锡的变质沉积物重熔形成二长花岗岩, 导致白干湖晚志留世岩浆热液型钨锡矿床形成。

致谢: 研究工作得到新疆地质调查局董连慧总工和屈迅教授等指导, 野外工作期间得到新疆地调院和吉林省地调院及下属单位的热情帮助, 测试工作得到北京大学造山带与地壳演化教育部重点实验室季建清老师、周晶老师、涂继耀博士等指导与帮助, 审稿专家提出了宝贵修改意见, 在此一并致谢。

参考文献(References):

[1] 姜春发, 冯秉贵, 杨经绥, 等. 昆仑地质构造轮廓[J]. 中国地质科学院地质研究所所刊, 1986, 15: 70−80.
Jiang Chunfa, Feng Binggui, Yang Jingsui, et al. An outline on the tectonics of the Kunlun region[J]. Bulletin of the Institute of Geology, Chinese Academy of Geological Sciences, 1986, 15: 70−80 (in Chinese with English abstract).

[2] 朱松年. 中国西部阿祁昆地区的构造演化[J]. 长春地质学院学报, 1986, 3: 41−52.
Zhu Songnian. The tectonic evolution of AQK area, Western China. Journal of Changchun Geology College, 1986, 3: 41− 52 (in Chinese with English abstract).

[3] 潘桂棠. 全球洋−陆转换中的特提斯演化[J]. 特提斯地质, 1994, 18: 23−40.
Pan Guitang. An evolution of Tethys in Global ocean− continent transformation[J]. Tethyan Geology, 1994, 18: 23−40 (in Chinese with English abstract).

[4] Yang J S, Robinson P T, Jiang C F, et al. Ophiolites of the Kunlun mountains, China and their tectonic implications[J]. Tectonophysics, 1996, 258: 299−305.

[5] Yin A, Harrison T M. Geologic evolution of the Himalayan−Tibetan Orogen[J]. Annual Review of Earth and Planetary Sciences, 2000, 28: 211−280.

[6] 边千韬, 赵大升, 叶正仁, 等. 初论昆祁秦缝合系[J]. 地球学报, 2002, 23(6): 501−508.
Bian Qiantao, Zhao Dasheng, Ye Zhengren, et al. A preliminary study of the Kunlun− Qilian− Qinling suture system[J]. Acta Geoscientia Sinica, 2002, 23(6): 501−508 (in Chinese with English abstract).

[7] 任纪舜. 昆仑−秦岭造山系的几个问题[J]. 西北地质, 2004, 37(1): 1−5.
Ren Jishun. Some problems on the Kunlun− Qinling orogenic system[J]. Northwestern Geology, 2004, 37(1): 1− 5 (in Chinese with English abstract).

[8] 杨经绥, 许志琴, 李海兵, 等. 东昆仑阿尼玛卿地区古特提斯火山作用和板块构造体系[J]. 岩石矿物学杂志, 2005, 24(5): 369−380.
Yang Jingsui, Xu Zhiqin, Li Haibing, et al. The Paleo− Tethyan volcanism and plate tectonic regime in the A'nyemaqen region of East Kunlun, northern Tibet Plateau[J]. Acta Petrologica et Mineralogica, 2005, 24(5): 369− 380 (in Chinese with English

abstract).

[9] 陈能松, 孙敏, 王勤燕, 等. 东昆仑造山带中带的锆石U−Pb定年与构造演化启示[J]. 中国科学(D辑), 2008, 38(6): 657−666.
Chen Nengsong, Sun Min, Wang Qinyan, et al. U− Pb dating of zircon from the Central East Kunlun Orogen and its implication for tectonic evolution[J]. Science in China (Ser. D), 2008, 38(6): 657−666 (in Chinese).

[10] 许志琴, 杨经绥, 姜枚, 等. 青藏高原北部东昆仑—羌塘地区的岩石圈结构及岩石圈剪切断层[J]. 中国科学D辑, 2001, 31(增刊): 1−7 (in Chinese).
Xu Zhiqin, Yang Jingsui, Jiang Mei, et al. Lithosphere structure and lithospheric shear fault of East Kunlun, Qiangtang area north of the Qinghai− Tibet Plateau [J]. Science in China Series D− Earth Sciences, 31(S1), 1 (2001) 10.1360/zd2001− 31− S1− 1(in Chinese).

[11] 许志琴, 李思田, 张建新, 等. 塔里木地块与古亚洲/特提斯构造体系的对接[J]. 岩石学报, 2011, 27(1): 1−22.
Xu Zhiqin, Li Sitian, Zhang Jianxin, et al. Paleo− Asian and Tethyan tectonic systems with docking the Tarim block[J]. Acta Petrologica Sinica, 2011, 27(1): 1− 22 (in Chinese with English abstract).

[12] Hu Ruizhong, Wei Wenfeng, Bi Xianwu, et al. Molybdenite Re− Os and muscovite $^{40}Ar/^{39}Ar$ dating of the Xihuashan tungsten deposit, central Nanling district, South China[J]. Lithos, 2012, 150: 111−118.

[13] 高永宝, 李文渊. 东昆仑造山带祁漫塔格地区白干湖含钨锡矿花岗岩: 岩石学, 年代学, 地球化学及岩石成因[J]. 地球化学, 2011, 40(4): 324−336.
Gao Yongbao, Li Wenyuan. Petrogenesis of granites containing tungsten and tin ores in the Baiganhu deposit, Qimantag, NW China: Constraints from petrology, chronology and geochemistry[J]. Geochimica, 2011, 40(4): 324− 336 (in Chinese with English abstract).

[14] Gao Yongbao, Li Wenyuan, Li Zhiming, et al. Geology, geochemistry, and genesis of tungsten− tin deposits in the Baiganhu district, northern Kunlun belt, northwestern China[J]. Economic Geology, 2014, 109: 1787−1799.

[15] 曹勇华, 赖健清. 新疆白干湖钨锡矿流体包裹体特征及成因[J]. 中南大学学报(自然科学版), 2012, 43(2): 644−650.
Cao Yonghua, Lai Jianqing. Characteristics of fluid inclusions and ore genesis of Baiganhu tungsten− tin deposit, Xinjiang[J]. Journal of Central South University (Science and Technology), 2012, 43(2): 644−650(in Chinese with English abstract).

[16] 高永宝, 李文渊, 张照伟. 祁漫塔格白干湖—戛勒赛钨锡矿带石英脉型矿石流体包裹体及氢氧同位素研究[J]. 岩石学报, 2011, 27(6): 1829−1839.
Gao Yongbao, Li Wenyuan, Zhang Zhaowei. Fluid inclusions and H−O isotopic compositions of quartz−vein ores in the Baiganhu− Jialesai W−Sn mineralization belts, Qimantag, NW China[J]. Acta Petrologica Sinica, 2011, 27(6): 1829− 1839 (in Chinese with English abstract).

[17] Chai Peng, Sun Jinggui, Hou Zengqian, et al. Geological, fluid inclusion, H− O− S− Pb isotope, and Ar− Ar geochronology constraints in the genesis of the Nancha gold deposit, southern Jilin Province, northeast China[J]. Ore Geology Reviews, 2016, 72: 1053−1071.

[18] Sun Xiaoming, Wei Huixiao, Zhai Wei, et al. Fluid inclusion geochemistry and Ar− Ar geochrnonlogy of the Cenozoic Bangbu orogenic gold deposit, southern Tibet, China[J]. Ore Geology Reviews, 2016, 74: 196−210.

[19] Bray C J, Spooner E T C, Hall C M, et al. Laser probe $^{40}Ar/^{39}Ar$ and conventional K− Ar dating of illites associated with the McClean unconformity− related uranium deposits, north Saskatchewan, Canada[J]. Canadian Journal of Earth Science, 1987, 24: 10−23.

[20] Li Xiaofeng, Wang Guo, Mao Wei, et al. Fluid inclusions, muscovite Ar− Ar age, and fluorite trace elements at the Baiyanghe volcanic Be− U− Mo deposit, Xinjiang, northwest China: Implication for its genesis[J]. Ore Geology Reviews, 2015, 64: 387−399.

[21] Marsh Timothy M, Einaudi Marco T, Mcwillisms Michael. $^{40}Ar/^{39}Ar$ geochronology of Cu− Au and Au− Ag mineralization in the Potrerillos district, Chile[J]. Economic Geology, 1997, 92: 784− 905.

[22] Garnier Virginie, Giuliani Gaston, Maluski Henri, et al. Ar− Ar ages in phlogopites from marble−hosted ruby deposits in northern Vietnam: Evidence from Cenozoic ruby formation[J]. Chemical Geology, 2002, 188: 33−49.

[23] 彭建堂, 胡瑞忠, 毕献武, 等. 湖南芙蓉锡矿床$^{40}Ar/^{39}Ar$同位素年龄及地质意义[J]. 矿床地质, 2007, 26(3): 237−248.
Peng Jiantang, Hu Ruizhong, Bi Xianwu, et al. $^{40}Ar/^{39}Ar$ isotopic dating of tin mineralization in Furong deposit of Hunan Province and its geological significance[J]. Mineral Deposits, 2007, 26(3): 237−248 (in Chinese with English abstract).

[24] Guo Chunli, Mao Jingwen, Bierlein Frank, et al. SHRIMP U−Pb (zircon), Ar− Ar (muscovite) and Re− Os (molybdenite) isotope dating of the Taoxikeng tungsten deposit, South China Block[J]. Ore Geology Reviews, 2011, 43: 26−39.

[25] 袁顺达, 侯可军, 刘敏. 安徽宁芜地区铁氧化物−磷灰石矿床中金云母Ar−Ar定年及其地球动力学意义[J]. 岩石学报, 2010, 26(3): 797−808.
Yuan Shunda, Hou Kejun, Liu Ming. Timing of mineralization and geoodynamic framework of iron− oxide− apatite deposits in Ningwu Cretaceous basins in the Middle− lower Reaches of the Yangtze River, China: Constraints from Ar− Ar dating on Phlogopites[J]. Acta Petrologica Sinica, 2010, 26(3): 797−808 (in Chinese with English abstract).

[26] Zhang Rongqing, Lu Jianjun, Wang Rucheng, et al. Constraints of

in situ zircon and cassiterite U−Pb, molybdenite Re−Os and muscovite $^{40}Ar/^{39}Ar$ ages on multiple generations of granitic magmatism and related W−Sn mineralization in the Wangxianling area, Nanling Range, South China[J]. Ore Geology Reviews, 2015, 65: 1021−1042.

[27] 姜春发. 昆仑开合构造[M]. 北京: 地质出版社, 1992: 1−320.
Jiang Chunfa. Opening− Closing Tectonics of the Kunlun Mountains[M]. Beijing: Geological Publishing House, 1992: 1−320 (in Chinese with English abstract).

[28] 李荣社, 计文化, 杨永成, 等. 昆仑山及邻区地质[M]. 北京: 地质出版社, 2008: 1−400.
Li Rongshe, Ji Wenhua, Yang Yongcheng, et al. Geology of Kunlun Mountain and Adjacent Area[M]. Beijing: Geological Publishing House, 2008: 1−400 (in Chinese).

[29] 王向利, 高小平, 刘幼骐, 等. 东昆仑祁漫塔格群的重新厘定[J]. 西北地质, 2010, 43(4): 168−178.
Wang Xiangli, Gao Xiaoping, Liu Youqi, et al. Revision of the Qimantag Group in west part of East Kunlun[J]. Northwestern Geology, 2010, 43(4): 168− 178 (in Chinese with English abstract).

[30] 高晓峰, 校培喜, 贾群子. 滩间山群的重新厘定[J]. 地质学报, 2011, 85(9): 1452−1463.
Gao Xiaofeng, Xiao Peixi, Jia Qunzi. Redetermination of the Tanjianshan Group: Geochronological and geochemical evidence of basalts from the margin of the Qaidam basin[J]. Acta Geologica Sinica, 2011, 85(9): 1452− 1463 (in Chinese with English abstract).

[31] 陈有炘, 裴先治, 李瑞保, 等. 东昆仑造山带东段元古界小庙岩组的锆石U−Pb年龄[J]. 现代地质, 2011, 25(3): 510−521.
Chen Youxin, Pei Xianzhi, Li Ruibao, et al. Zircon U−Pb age of Xiaomiao Formation of Proterozoic in the eastern section of the East Kunlun orogenic belt[J]. Geoscience, 2011, 25(3): 510− 521 (in Chinese with English abstract).

[32] 王国灿, 魏启荣, 贾春兴, 等. 关于东昆仑地区前寒武纪地质的几点认识[J]. 地质通报, 2007, 26(8): 929−937.
Wang Guocan, Wei Qirong, Jia Chunxing, et al. Some ideas of Precambrian geology in the East Kunlun, China[J]. Geological Bulletin of China, 2007, 26(8): 929−937 (in Chinese with English abstract).

[33] 黎敦朋, 樊晶, 肖爱芳, 等. 东昆仑西段祁漫塔格群早志留世笔石化石的发现[J]. 地质通报, 2002, 21(3): 136−139.
Li Dunpeng, Fan Jing, Xiao Aifang, et al. Discovery of Early Siluian graptolite fossils in the Qimantag Group in the western sector of the East Kunlun[J]. Geological Bulletin of China, 2002, 21(3): 136−139 (in Chinese with English abstract).

[34] 黎敦朋, 李新林, 周小康, 等. 阿牙克库木湖幅地质调查新成果及主要进展[J]. 地质通报, 2004, 23(5/6): 590−594.
Li Dunpeng, Li Xinlin, Zhou Xiaokang, et al. New results and major progress in regional geological survey of the Ayakkum Lake sheet[J]. Geological Bulletin of China, 2004, 23(5/6): 590−594 (in Chinese with English abstract).

[35] 赵振明, 李荣社, 计文化, 等. 志留纪昆仑山地区构造古地理环境及其成矿意义[J]. 中国地质, 2010, 37(5): 1284−1304.
Zhao Zhenming, Li Rongshe, Ji Wenhua, et al. Silurian tectonic−paleogeographic environment in Kunlun Mountain area and its metallogenic significance[J]. Geology in China, 2010, 37(5): 1284−1304 (in Chinese with English abstract).

[36] 陆露, 吴珍汉, 胡道功, 等. 东昆仑牦牛山组流纹岩锆石U−Pb年龄及构造意义[J]. 岩石学报, 2010, 26(4): 1150−1158.
Lu Lu, Wu Zhenhan, Hu Daogong, et al. Zircon U−Pb age for rhyolite of the Maoniushan Formation and its tectonic significance in the East Kunlun Mountain[J]. Acta Petrologica Sinica, 2010, 26(4): 1150− 1158 (in Chinese with English abstract).

[37] 尹福光, 潘桂棠. 东昆仑西段晚古生代盆地系[J]. 地球学报, 2008, 29(1): 31−38.
Yin Fuguang, Pan Guitang. The Late Paleozoic basin systems in the western part of East Kunlun[J]. Acta Geoscientica Sinica, 2008, 29(1): 31−38 (in Chinese with English abstract).

[38] 李瑞保, 裴先治, 李佐臣, 等. 东昆仑东段晚古生代—中生代若干不整合面特征及其对重大构造事件的响应[J]. 地学前缘, 2012, 19(5): 244−254.
Li Ruibao, Pei Xianzhi, Li Zuochen, et al. Geological characteristics of Late Paleozoic− Mesozoic unconformities and their response to some significant tectonic events in eastern part of Eastern Kunlun[J]. Earth Science Frontiers, 2012, 19(5): 244−254 (in Chinese with English abstract).

[39] 肖爱芳. 东昆仑祁漫塔格山西段鸭子泉志留纪火山岩特征[J]. 陕西地质, 2005, 23(2): 50−60.
Xiao Aifang. Yaziquan Silurian volcanic rocks in western Qimantahe Mountain of eastern Kunlun[J]. Shaan'xi Geology, 2005, 23(2): 50−60 (in Chinese with English abstract).

[40] 崔美慧, 孟繁聪, 吴祥柯. 东昆仑祁漫塔格早奥陶世岛弧: 中基性火成岩地球化学, Sm−Nd同位素及年代学证据[J]. 岩石学报, 2011, 27(11): 3365−3379.
Cui Meihui, Meng Fancong, Wu Xiangke. Early Ordovician island arc of Yaziquan, west of Qimantag Mountain, Eastern Kunlun: Evidences from geochemistry, Sm− Nd isotopes and geochronology of intermediate− basic igneous rocks[J]. Acta Petrologica Sinica, 2011, 27(11): 3365− 3379 (in Chinese with English abstract).

[41] 于文杰, 薛连明. 略论祁漫塔格地质构造特征[J]. 西北地质, 1986, (3): 17−23.
Yu Wenjie, Xue Lianming. Remarks on the geological structure characteristics of Qimantag[J]. Northwestern Geology, 1986, (3): 17−23 (in Chinese with English abstract).

[42] 郭通珍, 谈生祥, 常革红, 等. 祁漫塔格韧性剪切带中绢云母$^{40}Ar/^{39}Ar$定年及地质意义[J]. 西北地质, 2012, 45(1): 94−101.

Guo Tongzhen, Tan Shengxiang, Chang Gehong, et al. $^{40}Ar/^{39}Ar$ dating of the muscovite in the sericite of the Qimantag ductile shear zone and its geological significance[J]. Northwestern Geology, 2012, 45(1): 94−101 (in Chinese with English abstract).

[43] 陈丹玲, 刘良, 车自成, 等. 祁漫塔格印支期A型花岗岩的确定及初步研究[J]. 地球化学, 2001, 30(6): 540−546.
Chen Danling, Liu Liang, Che Zicheng, et al. Determination and preliminary study of Indosinian aluminous A−type granites in the Qimantag area, southeastern Xinjiang[J]. Geochimica, 2001, 30 (6): 540−546 (in Chinese with English abstract).

[44] 张亚峰, 裴先治, 丁仨平, 等. 东昆仑都兰县可可沙地区加里东期石英闪长岩锆石LA−ICP−MS U−Pb年龄及其意义[J]. 地质通报, 2010, 29(1): 79−85.
Zhang Yafeng, Pei Xianzhi, Ding Saping, et al. LA− ICP− MS zircon U− Pb age of quartz diorite at the Kekesha area of Dulan County, eastern section of the East Kunlun orogenic belt, China and its significance[J]. Geological Bulletin of China, 2010, 29(1): 79−85 (in Chinese with English abstract).

[45] 吴祥柯, 孟繁聪, 许虹, 等. 青海祁漫塔格玛兴大坂晚三叠世花岗岩年代学, 地球化学及Nd− Hf同位素组成[J]. 岩石学报, 2011, 27(1): 3380−3394.
Wu Xiangke, Meng Fancong, Xu Hong, et al. Zircon U− Pb dating, geochemistry and Nd− Hf isotopic compositions of the Maxingdaban Late Triassic granitic pluton from Qimantag in the eastern Kunlun[J]. Acta Petrologica Sinica, 2011, 27(1): 3380−3394 (in Chinese with English abstract).

[46] 李洪茂, 时友东, 刘忠, 等. 东昆仑若羌地区白干湖钨锡矿床地质特征及成因[J]. 地质通报, 2006, 25(1/2): 277−281.
Li Hongmao, Shi Youdong, Liu Zhong, et al. Geological features and origin of the Baiganhu W− Sn deposit in the Ruoqiang area, East Kunlun mountains, China[J]. Geological Bulletin of China, 2006, 25(1/2): 277−281 (in Chinese with English abstract).

[47] Chen Yanjing, Chen Huayong, Zaw Khin, et al. 2007. Geodynamic settings and tectonic model of skarn gold deposits in China: An overview[J]. Ore Geology Reviews, 31, 139−169.

[48] Chen Y J, Santosh M, Somerville I, et al. Indosinian tectonics and mineral systems in China: an introduction[J]. Geol. J. , 2014, 49, 331−337.

[49] 李大新, 丰成友, 周安顺, 等. 东昆仑祁漫塔格西段白干湖超大型钨锡矿田地质特征及其矿化交代岩分类[J]. 矿床地质, 2013, 32(1): 37−54.
Li Daxin, Feng Chengyou, Zhou Anshun, et al. Geological characteistics and mineralizations− metasomatite classification of superlarge Baiganhu tungsten− tin orefield in western Qimantag, East Kunlun mountain[J]. Mineral Deposits, 2013, 32(1): 37− 54 (in Chinese with English abstract).

[50] Ludwig Kenneth R. ISOPLOT 3. 00: A Geochronological Toolkit for Microsoft Excel [M]. Berkeley Geochronology Center Special Publication. 2003, No. 4: 170.

[51] Dalrymple G Brent, Lamphere Marvin A. $^{40}Ar/^{39}Ar$ tectonique of K− Ar dating: a comparison with the conventional technique[J]. Earth and Planetary Science Letters, 1971, 12: 300−308.

[52] Hanson Gilbert N, Smimons Kathleen R, Bence A E. $^{40}Ar/^{39}Ar$ spectrum ages for biotite, hornblende and muscovite in a contract metamorphic zone [J]. Geochim. Cosmochim. Acta, 1975, 39: 1269−1277.

[53] 邱华宁, 彭良. $^{40}Ar/^{39}Ar$年代学与流体包裹定年[M]. 合肥: 中国科学技术大学出版社, 1997: 1−242.
Qiu Huaning, Peng Liang. $^{40}Ar/^{39}Ar$ Geochronology and Fluid Inclusion Dating[M]. Hefei: Press of University of Science and Technology of China, 1997: 1−242 (in Chinese).

[54] 陈文, 万渝生, 李华芹, 等. 同位素地质年龄测定技术及应用[J]. 地质学报, 2011, 85(11): 1917−1946.
Chen Wen, Wan Yusheng, Li Huaqin, et al. Isotope Geochronology: Technique and application[J]. Acta Geologica Sinica, 2011, 85(11): 1917− 1946 (in Chinese with English abstract).

[55] Lanphere Marvin A, Dalrymple G Brent. A test of the $^{40}Ar/^{39}Ar$ age spectrum technique on some terrestrial materials[J]. Earth Planet. Sci. Lett. 1971, 12: 359−372.

[56] Roddick J C, Cliff R A, Rex D C. The evolution of excess argon in alpine biotites——A $^{40}Ar/^{39}Ar$ analysis[J]. Earth Planet. Sci. Lett., 1980, 48: 185−208.

[57] Harrison T Mark, McDougall Ian. Excess ^{40}Ar in metamorphic rocks from Broken Hill, New South Wales: Implications for $^{40}Ar/^{39}Ar$ age spectra and the thermal history of the region[J]. Earth Planet. Sci. Lett. 1981, 55: 123−149.

[58] Harrison T Mark. Some observations on the interpretation of $^{40}Ar/^{39}Ar$ age spectra[J]. Chemical Geology, 1983, 41: 319−338.

[59] Faure Gunter, Mensing Teresa M. Isotopes: Principles and Applications[M]. Canada: John Wiley and Sons, Inc. , Hoboken, New Jersey. 2005: 144−179.

[60] Yuan Shunda, Peng Jiantang, Shen Nengping, et al. $^{40}Ar/^{39}Ar$ isotopic dating of the Xianghualing Sn− polymetallic orefield in southern Hunan, China and its geological implications [J]. ActaGeologicaSinica, 2007, 81(2): 278−286.

[61] 谢桂青, 毛景文, 李瑞玲, 等. 鄂东南地区大型矽卡岩型铁矿床金云母$^{40}Ar/^{39}Ar$同位素年龄及其构造背景初探[J]. 岩石学报, 2008, 24(8): 1917−1927.
Xie Guiqing, Mao Jinwen, Li Ruiling, et al. $^{40}Ar/^{39}Ar$ phlogopite dating of large skarn Fe deposits and tectonic framework in southeastern Hubei Province, Middle− Lower Reaches of the Yangtze River, eastern China[J]. Acta Petrologica Sinica, 2008, 24 (8): 1917−1927 (in Chinese with English abstract).

[62] Selby David, Creaser Robert A, Hart Craig J R, et al. Absolute timing of sulfide and gold mineralization: A comparison of Re− Os molybdenite and Ar− Ar mica methods from the Tintina gold belt, Alaska [J]. Geology, 2002, 30: 791−794.

[63] 郑建民, 谢桂青, 刘珺, 等. 河北省南部邯郸—邢台地区西石门矽卡岩型铁矿床金云母$^{40}Ar/^{39}Ar$定年及意义[J]. 岩石学报, 2007, 23(10): 2513−2518.
Zheng Jianmin, Xie Guiqing, Liu Jun, et al. $^{40}Ar/^{39}Ar$ dating of phologopite from the Xishimen skarn iron deposit in the Handan−Xingtai area, southern Hebei, and its implications[J]. Acta Petrologica Sinica, 2007, 23(10): 2513− 2518 (in Chinese with English abstract).

[64] Peng Jiantang, Zhou Meifu, Hu Ruizhong, et al. Precise molybdenite Re− Os and mica Ar− Ar dating of the Mesozoic Yaogangxian tungsten deposit, central Nanling district, South China[J]. Mineralium Deposita, 2006, 41(7): 661−669.

[65] 白秀娟, 王敏, 卢克豪, 等. 锡石$^{40}Ar/^{39}Ar$法直接定年探讨[J]. 科学通报, 2011, 56(23): 1899−1904.
Bai Xiujuan, Wang Min, Lu Kehao, et al. Direct dating of cassiterite by $^{40}Ar/^{39}Ar$ progressive crushing[J]. Chinese Sci. Bull., 2011, 56(23): 1899−1904 (in Chinese).

[66] Clauer Norbert. The K− Ar and $^{40}Ar/^{39}Ar$ methods revisited for dating fine− grained K− bearing clay minerals[J]. Chemical Geology, 2013, 354: 163−185.

[67] Purdy John W, Jäger Emilie. K− Ar ages on rocks forming minerals from the Central Alps[C]//MemoriedegliIstituti di Geologiae Mineralogiadell'Universita di Padova. 1976, 30: 1−321.

[68] Zheng Zhen, Deng Xiaohua, Chen Hongjin, et al. Fluid sources and metallogenesis in the Baiganhu W−Sn deposit, East Kunlun, NW China: Insights from chemical and boron isotopic compositions of tourmaline[J]. Ore Geology Review, 2016, 72: 1129−1142.

[69] 包亚范, 刘延军, 王鑫春. 东昆仑西段巴什尔希花岗岩与白干湖钨锡矿床的关系[J]. 吉林地质, 2008, 27(3): 56−67.
Bao Yafan, Liu Yanjun, Wang Xinchun. Relations between Bashierxi granite, west Dongkunlun and Baiganhu tungsten− tin deposit[J]. Jilin Geology, 2008, 27(3): 56− 67 (in Chinese with English abstract).

[70] 刘子峰, 崔雅茹, 魏巍. 新疆东昆仑白干湖钨锡矿床地球化学特征[J]. 吉林地质, 2007, 26(4): 54−60.
Liu Zifeng, Cui Yaru, Wei Wei. The geochemical characteristics of the Baiganhu W, Sn deposit, Dongkunlun, Xinjiang[J]. Jinlin Geology, 2007, 26(4): 54−60 (in Chinese with English abstract).

[71] Torsvik T H, Smethurst M A, Meert J G, et al. Continental breakup and collision in the Neoproterozoic and Paleozoic− a tale of Baltica and Laurentia[J]. Earth Sci. Rev. , 1996, 40: 229−258.

[72] Dalziel Ian W D. Neoproterozoic− Paleozoic geography and tectonics: Review, hypothesis and environmental speculation[J]. Geol. Soc. Amer. Bull. , 1997, 109: 16−42.

[73] 陆松年, 于海峰, 金巍, 等. 塔里木古大陆东缘的微大陆块体群[J]. 岩石矿物学杂志, 2002, 21(4): 317−326.
Lu Songnian, Yu Haifeng, Jin Wei, et al. Microcontinents on the eastern margin of Tarim paleocontinent[J]. Acta Petorlogica et Mineralogica, 2002, 21(4): 317− 326 (in Chinese with English abstract).

[74] 陆松年, 李怀昆, 陈志宏, 等. 新元古时期中国古大陆与罗迪尼亚超大陆的关系[J]. 地学前缘, 2004, 11(2): 515−523.
Lu Songnian, Li Huaikun, Chen Zhihong, et al. Relationship between Neoproterozic cratons of China and the Rodinia[J]. Earth Science Frontiers, 2004, 11(2): 515−523 (in Chinese with English abstract).

[75] Li Z X, Bogdanova S V, Collins A S, et al. Assembly, configuration, and break− up history of Rodinia: a synthesis[J]. Precambrian Research, 2008, 160: 179−210.

[76] Bogdanova S V, Pisarevsky S A, Li Z X. Assembly and breakup of Rodinia (some results of IGCP project 440) [J]. Stratigraphy and Geological Correlation, 2009, 17: 259−274.

[77] Meng Fancong, Cui Meihui, Wu Xiangke, et al. Heishan mafic− ultramafic rocks in the Qimantag area of Eastern Kunlun, NW China: Remnants of an early Paleozoic incipient island arc[J]. Gondwana Research, 2015, 27: 745−759.

[78] 潘裕生, 周伟明, 许荣华, 等. 昆仑山早古生代地质特征与演化[J]. 中国科学D辑, 1996, 26(4): 302−307.
Pan Yusheng, Zhou Weiming, Xu Ronghua, et al. Geological characteristics and evolution of Early Paleozoic in Kunlun mountains[J]. Science in China (Series D), 1996, 26(4): 302−307 (in Chinese).

[79] Pirajno Franco. The geology and tectonic settings of China's mineral deposits[C]//Chiapter 6 Tianshan, Junggar and Altay Orogens (NW China), the Alpine−Himalayan Fold Belts (Tethyan Orogens), Kunlun and Songpan−Ganzi Terranes. 2008: 381−545.

[80] 刘彬, 马昌前, 蒋红安, 等. 东昆仑早古生代洋壳俯冲与碰撞造山作用的转换: 来自胡晓钦镁铁质岩石的证据[J]. 岩石学报, 2013, 29(6): 2093−2106.
Liu Bin, Ma Changqian, Jiang Hongan, et al. Early Paleozoic tectonic transition from ocean subduction to collisional orogeny in the Eastern Kunlun region: Evidence from Huxiaoqin mafic rocks[J]. Acta Petrologica Sinica, 2013, 29(6): 2093− 2106 (in Chinese with English abstract).